PROCEEDINGS OF SCIENCE

The CMS Experiment: Status and Highlights

Guido Tonelli for the CMS Collaboration

CERN, INFN and University of Pisa

CERN, European Organization for Nuclear Research
CH-1211 Geneva 23, Switzerland

Abstract

We present the status of the CMS experiment at the LHC and the highlights of its first physics results. Using pp collisions at centre-of-mass energy of 7 TeV, about 303nb^{-1} of integrated luminosity have been collected by CMS out of a total of about 346nb^{-1} delivered by LHC. We report on the performance of the trigger and the data acquisition systems, on the commissioning of the main detector components and on the physics objects and tools.
The first physics measurements performed on these data are then described. We present results on charged hadrons multiplicities, inclusive jet cross section and measurements of the J/ψ and ϒ differential cross section as a function of p_T. We then show results on W and Z bosons, including measurements of their production cross sections. Lastly we present the first observation of top quark pairs produced at the LHC and identified both in single-lepton and di-lepton decay channels.

E-mail: guido.tonelli@cern.ch

PoS(ICHEP 2010)565

1. Introduction

The Compact Muon Solenoid (CMS) is one of the two "general-purpose" detectors at the Large Hadron Collider [1]. It is located at the experimental Point 5 of the LHC near Cessy (France).
The main distinguishing features of CMS are (Fig.1) a large superconducting solenoid magnet, which creates a strong field of 3.8 Tesla, a state-of-the-art silicon tracker, a highly granular crystal electromagnetic calorimeter, fully hermetic hadronic calorimeters and a sophisticated and redundant muon system. The detector has been built thanks to the collective effort of the CMS Collaboration consisting of more than 3170 scientists and engineers from 182 Institutes distributed in 39 countries all over the world.

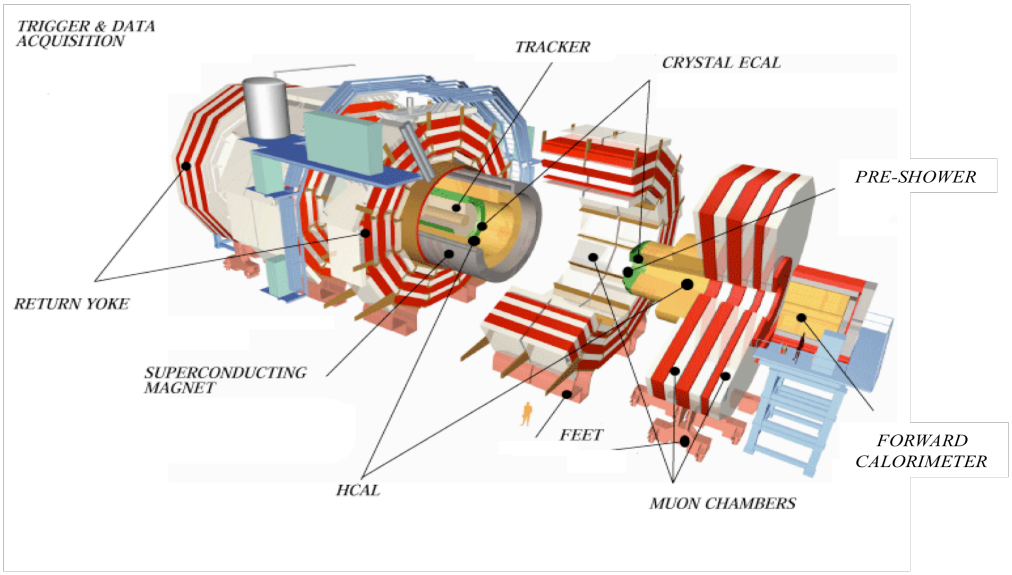

Fig. 1. Schematic view of the CMS detector.

Prior to collecting pp collisions the detector has been thoroughly calibrated using muons produced in cosmic rays. A large data set of more than 10^9 muons was recorded in successive campaigns of cosmic ray data taking in 2008 and 2009. As a result of these studies it was possible to achieve a good understanding of the initial alignment constants of the major detector components and a detailed map of the magnetic field. They led to an excellent control of the momentum resolution and absolute scale. The commissioning of the detector was then completed using the first LHC pilot runs at 0.9 and 2.36TeV collision energies at the end of 2009.

2. LHC and CMS 7TeV Operations

The LHC started 7TeV operations in spring 2010, at very low luminosity, in the range of $\mathcal{L}=10^{27}\text{cm}^{-2}\text{s}^{-1}$, but reached very quickly instantaneous luminosities exceeding $\mathcal{L}=10^{30}\text{cm}^{-2}\text{s}^{-1}$. In total an integrated luminosity of ~346nb^{-1} has been delivered so far by the LHC. CMS has collected about 303nb^{-1} of data corresponding to an overall data-taking efficiency of about 88%. It is worth noticing that about 2/3 of the total integrated luminosity has been delivered in the last week just before the start of this conference. The quality of the data taken so far is quite good:

$280nb^{-1}$ of data is considered good for muon-based analyses while $254nb^{-1}$ of data is validated for any analysis. An 11% uncertainty is currently estimated on the luminosity mainly due to the uncertainty on the number of protons in each bunch [2].
The overall operational status of CMS during this data taking was excellent. All sub-systems had a fraction of operational channels exceeding 98%. This is an outstanding achievement, especially since the total amount of read-out channels in CMS that is about 80 million.
CMS uses a two-stage trigger. The Level 1 is implemented in hardware and, for the current data taking, reduces the rate to a maximum of 45 kHz, including 22kHz of random triggers. The typical timing precision of all critical trigger components is 1ns or less. All Level 1 triggers have high efficiency and sharp turn-on curves. A couple of examples are shown in Fig.2.
The second stage of the CMS trigger, High Level Trigger (HLT) is fully implemented in software. In the first few weeks at low luminosities we collected essentially all the interactions that the LHC delivered. As collision rates started to exceed our offline data processing capabilities (300-500 Hz), we kept the L1 trigger open (triggering on all interactions) and required the High Level Trigger (HLT) to select the most interesting events. We adjusted the HLT triggers as the luminosity rose continuously to allow CMS to maximize the data collection for both high p_T (W, Z, tt…) and low p_T (J/ψ, ϒ, inclusive b…) physics.

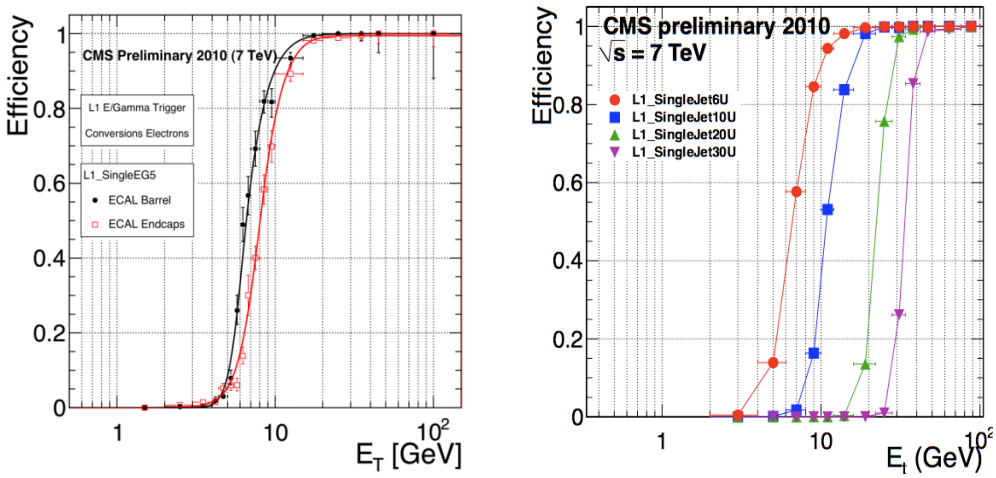

Fig. 2. Turn-on curves of the Level-1 trigger efficiency plotted against the reconstructed transverse energy for the electron/gamma trigger with 5GeV nominal threshold (left) and for jet triggers with several different thresholds (right).

Different HLT menus have been successfully deployed to cope with increasing instantaneous luminosities up to $1.6x10^{30}cm^{-2}s^{-1}$. A safety factor of 2 was always incorporated in the evaluation of the maximum sustainable rate. The processing time per event at the maximum luminosity faced so far ($\sim10^{30}cm^{-2}s^{-1}$) was ~50ms. The current farm capacity allows ~100ms/evt at a L1 rate of 50kHz. The average event size at the DAQ was about 500kB/evt. A total of 200-400Hz of data was sent for permanent storage on disks. Special HLT trigger paths were used to collect large statistics of π^os to calibrate the electromagnetic calorimeter with the goal to achieve a relative calibration among crystals better than 1%. Since the HLT is fully based on software it allows an enormous flexibility. New ideas or new trigger paths that could maximize the physics outcome of the experiment might be implemented and validated in a few weeks. This happened already in the current data taking, where, for example, two complementary algorithms were deployed to enrich significantly the J/ψ dataset. We estimate that the two triggers combined would be able to select ~50k J/ψ per pb^{-1} of collected data down to p_T =0 in the forward region.

The computing Tier-0 infrastructure was able to repack and promptly reconstruct collision data. The Tier-0 was able to reconstruct the express stream (~10% of the data) within an hour and also quickly reconstruct the entire data accumulated, storing it and transferring physics-quality data to Tier-1s. The Tier-1s generally functioned very well throughout the run and efficiently served data to Tier-2s for analysis. In the week before ICHEP more than 500 individuals submitted analysis jobs to the Tier-2 centers. CMS offline software has been running smoothly throughout the data-taking period and keeping pace with the evolution of the luminosity delivered by LHC. Most of the analyses produced for ICHEP used data collected and analyzed with the latest CMS software release used at Tier-0 since June. The Physics Validation Team (PVT) produced good run and luminosity-section lists very quickly in order to have the maximum luminosity available for results. Some of the talks at this Conference used data collected just 36 hours prior to presentation time.

3. Detector Performance and Commissioning of the Major Physics Tools

After many years of detailed Monte-Carlo studies it was important to check first that the CMS detector is well understood and that resolutions and other features obtained from the analysis of collision data match the values derived from simulations. The speed by which these first results were obtained was unprecedented. It was mostly due to the fact that the alignment and calibration conditions of the detector were already in place thanks to excellent use and analysis of cosmic ray data taken in the previous two years.
All major detector systems performed very well. The MC description of the tracker performance matches extremely well the data. Fig. 3 shows the comparison between data and MC distributions of pseudo-rapidity and p_T of the reconstructed tracks [3]. Note the logarithmic scale of the latter plot, where an excellent agreement between data and MC extends over more than 5 orders of magnitude.

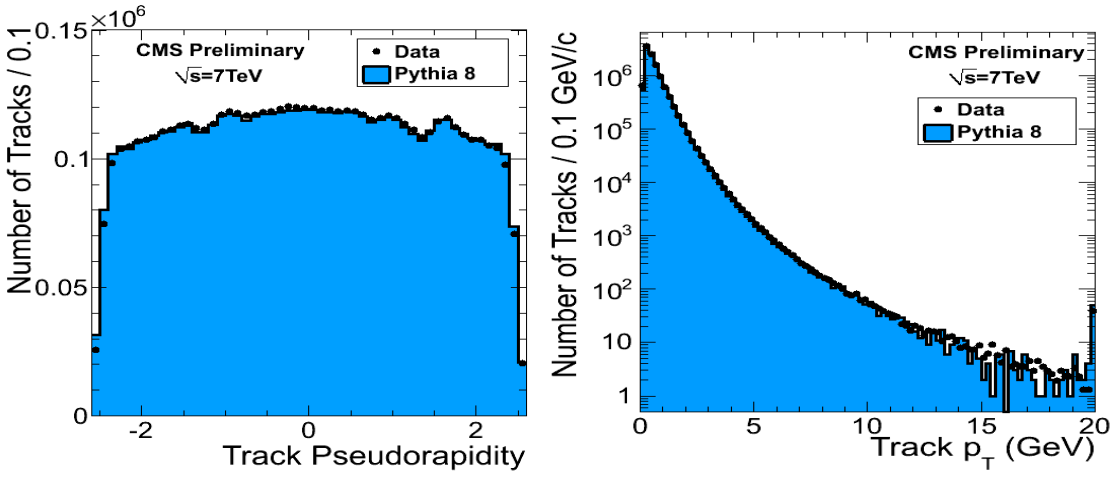

Fig. 3. Track pseudo-rapidity (left) and p_T (right) distributions.

The impressive status of the alignment and the general tracking performance allowed a quick validation of several different b-tagging algorithms. CMS currently uses four algorithms based on track counting, secondary vertex taggers, jet probability and lepton taggers [4]. For the first applications, high-efficiency and intermediate-purity taggers are preferred. Fig. 4 shows the excellent agreement between data and MC of the distributions of the 3D impact parameter (IP) significance. The plots are obtained using all tracks with p_T>1GeV/c inside jets with

p_T>40GeV/c and |η|<1.5. On the right hand side of the figure a zoom into the region of IP significance of 0±2 allows to better appreciate the details of the agreement.

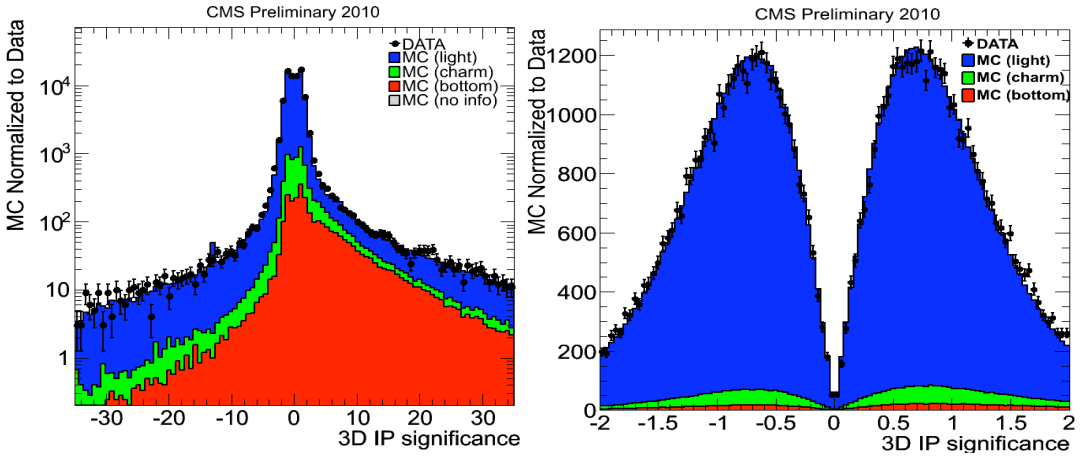

Fig. 4. Distribution of the 3D Impact Parameter Significance (left); zoom in the central region (|η|<1.5) of the same plot (right).

A comprehensive campaign is ongoing to study the tracker material budget. Several complementary methods are used: photon conversions, nuclear interactions and effects of multiple scattering on the precision measurements of low mass resonances. As a result of these studies we currently estimate that the uncertainty on the tracker material is less than 10%, which translates into a systematic uncertainty on physics quantities related to the tracker material budget of less than 1%.

The performance of the electromagnetic calorimeter has been studied in full detail. The distributions in η and ϕ of the electromagnetic clusters of electrons and photons show a remarkable agreement with MC simulation as well as the distribution of the energy. It is worth noticing that, by using first data, it has been possible to achieve a timing resolution of the barrel calorimeter better than 0.5ns.

Three different approaches are used in CMS to reconstruct jets. They differently combine individual contributions from various sub-detectors to form the inputs to the jet-clustering algorithm. The conventional approach (Calo-jets) is based on the purely calorimetric information; the Jet-Plus-Track approach (JPT-jets) uses the information on the charged particles associated to jets, as reconstructed by the tracker, to improve the measurements of the calorimeters; Particle-Flow (PFlow or PF-jets) is a completely new approach, specific to CMS, which combines all information available from the various sub-detectors. Jets are then reconstructed using the anti-k_T clustering algorithm with a cone size parameter R=0.5.

Jet energy measured in the detector is typically different from the corresponding particle jet energy. The latter is obtained in the simulation by clustering, with the same jet algorithm, the stable particles produced during the hadronization process that follows the hard interaction. The main cause for this energy mismatch is the non-uniform and non-linear response of the CMS calorimeters. Furthermore, electronics noise and additional pp interactions in the same bunch crossing (event pile-up) can lead to extra energy. The purpose of the jet energy correction (JEC) is to relate, on average, the energy measured in the detector to the energy of the corresponding particle jet. Following the approach of multi-step factorized jet energy calibration adopted by CMS, we have studied separately offset, relative and absolute jet energy corrections. Energy offset due to electronic noise and event pile-up has been estimated from Zero Bias and Minimum Bias trigger data. The di-jet p_T balance has been used to measure the jet response as a function of pseudo-rapidity, relative to the central region (|η| <1.3). The p_T balance and MPF

(Missing p_T Projection Fraction) methods in photon+jet events have been used to study the jet response in the central region as a function of jet p_T. Jet energy resolutions have been studied using asymmetry method in di-jet data events. The sample has also been used to study jet position resolutions. In general, better performance for jet types employing the tracking information have been observed compared to jets using calorimeter-only information.
Current physics analyses in CMS conservatively use 10% JEC uncertainties for calorimeter jets and 5% for JPT and PF-jets, with additional 2% uncertainty per unit rapidity [5].
The reconstruction of the missing transverse energy (MET) in the events is an important tool to address some of the most challenging physics goals of CMS like the search for Super-symmetry. We studied first the effect of instrumental anomalies and beam-induced backgrounds on the MET measurement and demonstrated a cleaning procedure to identify and correct for these effects. After the cleaning procedure, the distributions in the data are in general good agreement with Monte Carlo simulation predictions. The best resolution in missing transverse energy is obtained using Particle-Flow MET [6].

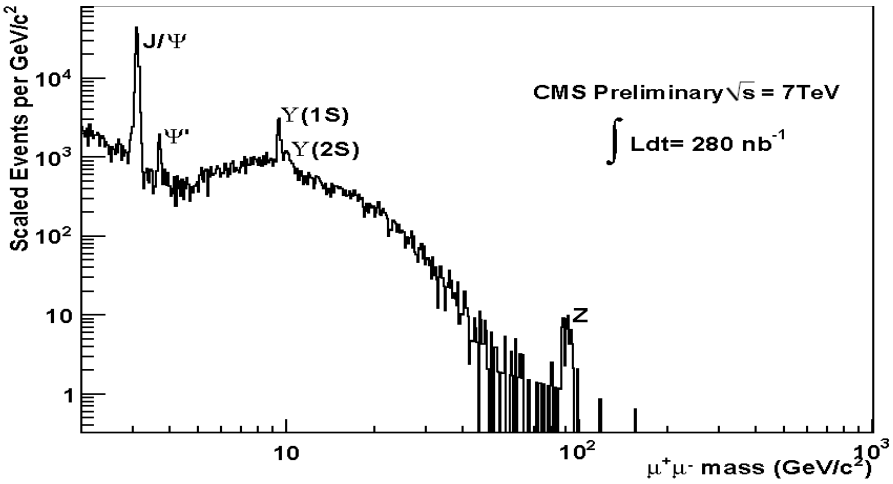

Fig. 5. Invariant mass distribution of particles decaying to $\mu^+\mu^-$ in CMS.

Following analysis of the cosmic data taken in 2008 and 2009, the performance of muon identification in CMS has been further studied on a sample of muons corresponding to an integrated luminosity of about $84nb^{-1}$. Measured distributions of basic muon-related quantities are well reproduced by the Monte Carlo simulation. Efficiencies of various high-level trigger, identification, and reconstruction algorithms have been measured in the muon momentum range up to about 15GeV/c, and found to agree within 5-10% of expectations. The probability to misidentify kaons or pions as muons due to their decay in flight agrees with predictions from simulation. The punch-through probability for tracks with momentum between 3 and 10GeV/c was measured to be $(5.3 \pm 0.8(\text{stat.}))\cdot 10^{-4}$, in agreement with expectations.
The excellent muon momentum resolution in CMS (less than 1% for muons in the central region, $|\eta| \leq 0.7$, and less than 3% for muons in the forward parts, $0.7 < |\eta| \leq 2.5$), can be appreciated when looking at the opposite-sign di-muon ($\mu^+\mu^-$) invariant mass distribution (Fig. 5). It has been obtained analyzing the full data set collected to far corresponding to $280nb^{-1}$. Well known members of the quarkonia families up to the Z boson are clearly visible. With the large statistics, soon to be available, we plan to calibrate precisely the CMS detector against known physics objects.

3.1 Soft QCD and Jet Physics

Using minimum bias events we have been able to measure the average transverse momentum and pseudo-rapidity distributions of charged tracks down to very low transverse momentum ($p_T \geq 50$MeV/c), in a large pseudo-rapidity interval ($|\Delta\eta| \leq 2.5$) for three different collision energies (0.9, 2.36 and 7TeV) [7]. The data are corrected for trigger and event selection efficiency, for effects of tracking inefficiency and secondary tracks originating from the decay of long-lived particles and for products of interactions with the beam pipe and the detector material. At higher energies we observe an increase in the density of particles in data stronger than in model predictions (Fig. 6). The results are being used as input to an improved Monte Carlo modeling of minimum bias events.

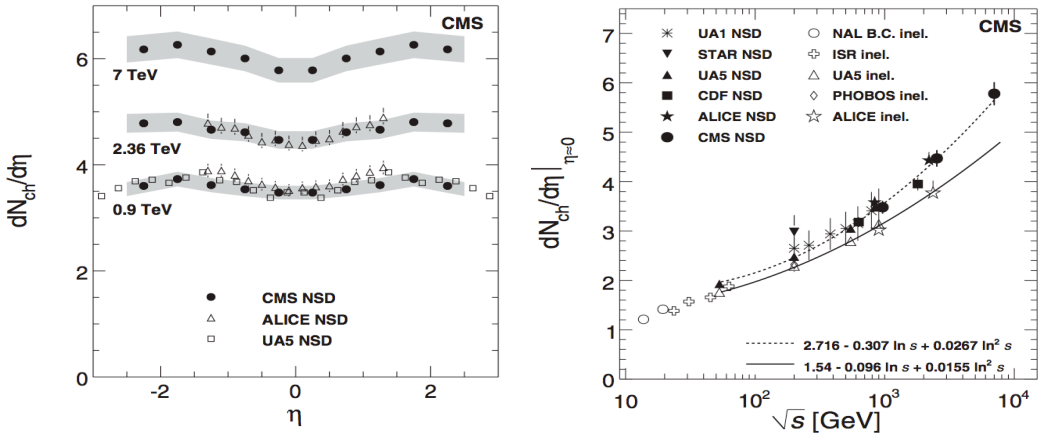

Fig. 6. Density of charged tracks in different η regions for collision energies 0.9, 2.36 and 7 TeV (left); average density of charged tracks in the very central region as a function of √s (right).

Inclusive jet p_T spectra have been produced for all three jet approaches used in CMS. The measured cross sections are found to be in agreement with next-to-leading order perturbative QCD calculations, within the experimental and theoretical uncertainties [8]. With the new Particle Flow approach the distributions can be extended to a low p_T value of 18 GeV/c (Fig.7).

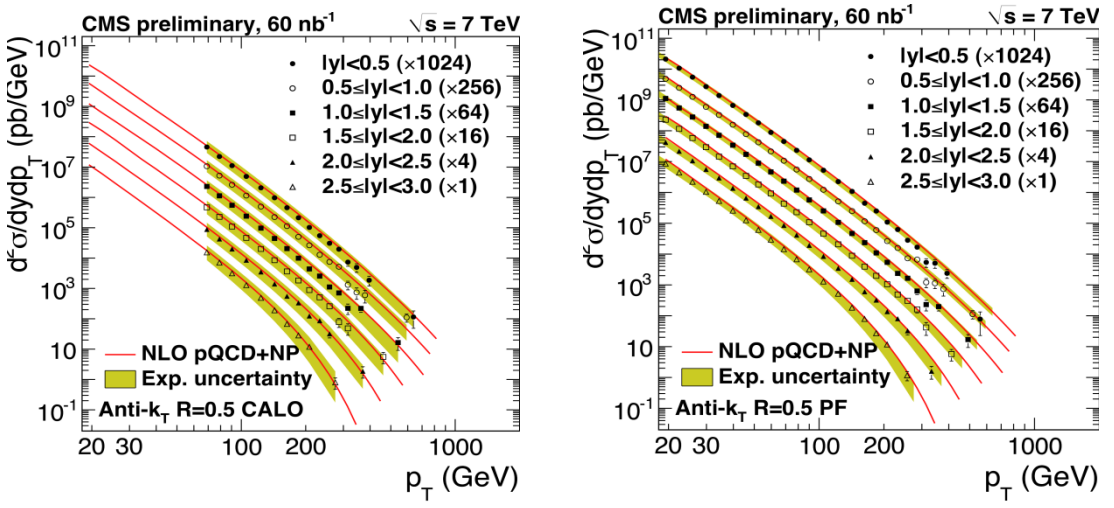

Fig. 7. Inclusive jet p_T spectra for purely calorimetric jets (left) and for particle flow jets (right).

Using 120nb^{-1} of data we have measured the di-jet mass differential cross section for centrally produced jets $|\eta_1, \eta_2|<1.3$ (Fig. 8). Since the distribution is very sensitive to the coupling of any new massive object to quarks and gluons we have been able to extract 95% exclusion limits on string resonances (1.67TeV), excited quarks (0.59TeV) and axigluons (0.52TeV) [9].

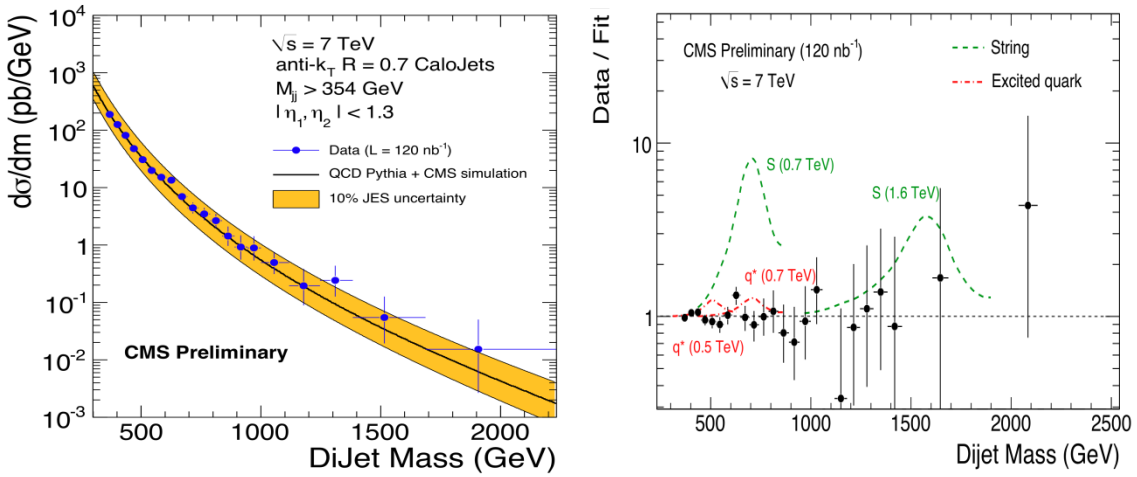

Fig. 8. Search for narrow resonances in di-jet final states. Di-jet mass distribution (left) and ratio of the data to the fit (right) with simulation of the signals due to new, heavy particles.

3.2 Quarkonia.

Using simple selection cuts in the di-muon data set it has been possible to identify a large sample of J/ψ and ϒ from which we have extracted the first measurements of the production cross sections at 7TeV.

The differential production cross section of J/ψ from inclusive processes has been measured as a function of the J/ψ transverse momentum, up to 30GeV/c, for two rapidity ranges: $|\eta| < 1.4$ and $1.4< |\eta| <2.4$ (Fig .9). The total cross section for inclusive J/ψ production, times the di-muon decay branching fraction, has been determined to be 289.1 ±16.7(stat)±60.1(syst) nb for $4 \le p_T \le 30$GeV/c and $|\eta|<2.4$.

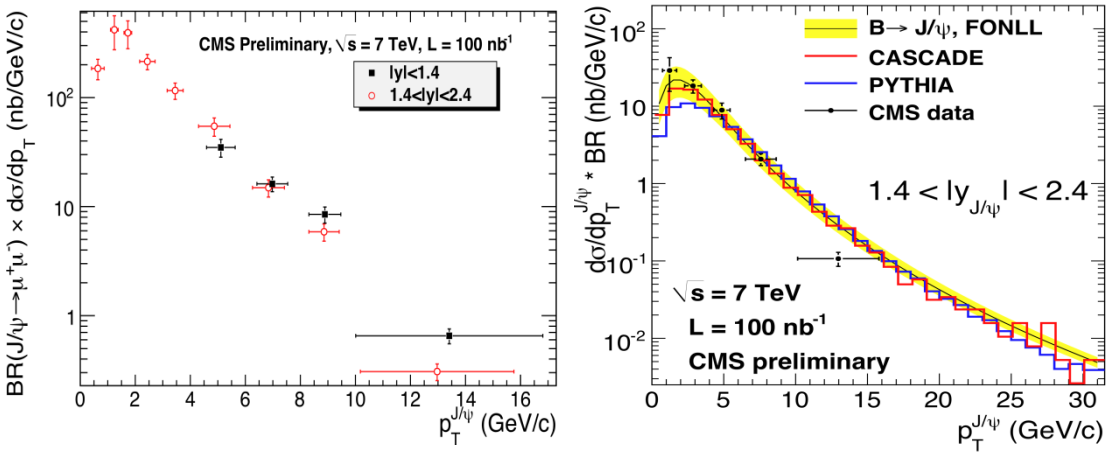

Fig. 9. J/ψ → $\mu^+\mu^-$ *differential cross sections: inclusive (left) and non-prompt (right).*

The b-hadron component has been extracted from a fit to the decay length distribution of displaced J/ψ decays, and a p_T differential cross section for b-hadron decays has been derived. The total cross section times BR($J/\psi \rightarrow \mu^+\mu^-$) for the J/ψ production coming from B-hadrons, for $4 \leq p_T \leq 30$GeV/c and $|\eta| < 2.4$ is measured to be 56.1±5.5(stat)±7.2 (syst) nb [10].
Lastly, we have measured the Υ(1S) cross section times BR to di-muons and the corresponding differential cross section integrated over $|y| < 2.0$. The result, assuming no polarization, yields $\sigma(pp \rightarrow \Upsilon(1S)+X) \cdot BR(\Upsilon(1S) \rightarrow \mu^+\mu^-) = 8.3 \pm 0.5(stat.) \pm 0.9(syst) \pm 1.0(lumi)$nb [11].

3.3 Intermediate Vector Bosons

The selection of W and Z bosons candidates in CMS decaying to muons starts from data collected using the inclusive muon HLT path: $\mu+X$ ($p_T^{\mu}>9$GeV/c) and $|\eta^{\mu}|<2$. For good quality muon track we require hits in the pixels, in the strip tracker and in the muon system as well as a reasonable overall fit (χ^2/dof <10). W candidates are selected requiring a relative isolation ≤0.15 in a cone of ΔR<0.3 around the muon. For the Z candidates we look for a second muon with looser quality criteria, opposite charge and $|\eta|<2.4$; both muons must be isolated with $p_T>20$GeV and invariant mass $60<m_{\mu\mu}<120$GeV/c^2. To extract the event yield we perform simultaneous fits to backgrounds and signal contributions. QCD background shapes are obtained using data while the EWK background shapes and signals are obtained from Monte Carlo simulations. Fig. 10 shows the results of the fits and the event yields: in 198nb^{-1} of data we have reconstructed 818±27 $W \rightarrow \mu\nu$ and 77 $Z(\gamma^*) \rightarrow \mu^+\mu^-$ candidates[12].

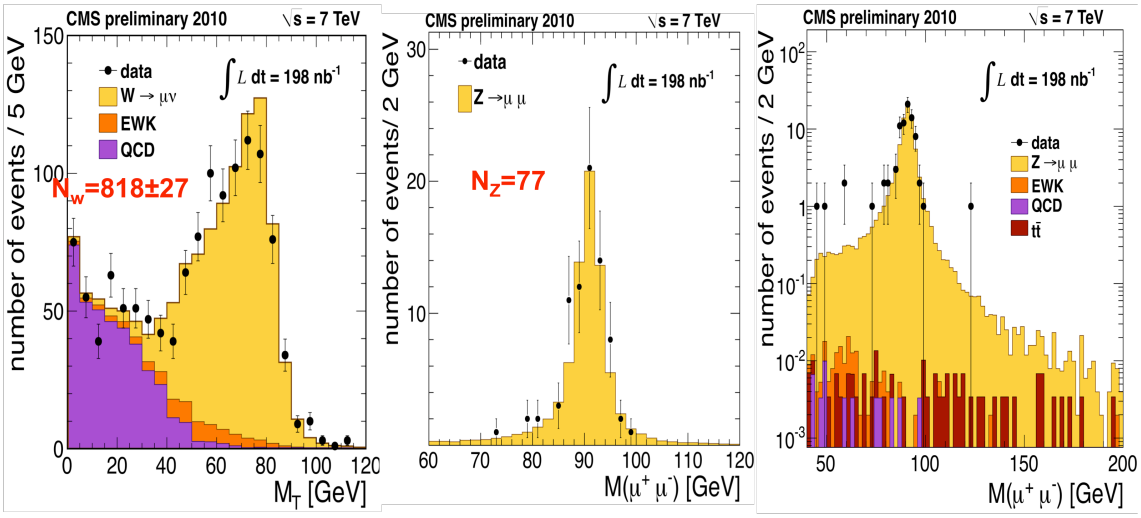

Fig. 10. Transverse mass distribution for $W \rightarrow \mu\nu$ (left) and invariant-mass distributions for $Z(\gamma^*) \rightarrow \mu^+\mu^-$ in linear (center) and logarithmic scale (right).

The HLT path for W and Z decaying to electrons is the inclusive $e/\gamma+X$ with E_T >15GeV. Events are then selected requiring $p_{Te}>20$GeV/c, $0<|\eta^e|<1.4$ or $1.566<|\eta^e|<2.5$. For the electron identification electromagnetic clusters are required to match a track and to pass certain cuts on the shower shape variables in ECAL and HCAL. A tight algorithm (75% efficiency) is used for the W candidates while a looser algorithm (90% efficiency) is used for the Z candidates. As in the case of muons, the yield of W bosons is determined using the simultaneous fits to the backgrounds and signal contributions. A total of 800±30 $W \rightarrow e\nu$ candidates are reconstructed in the data together with 61 $Z \rightarrow e^+e^-$ candidates (Fig. 11).

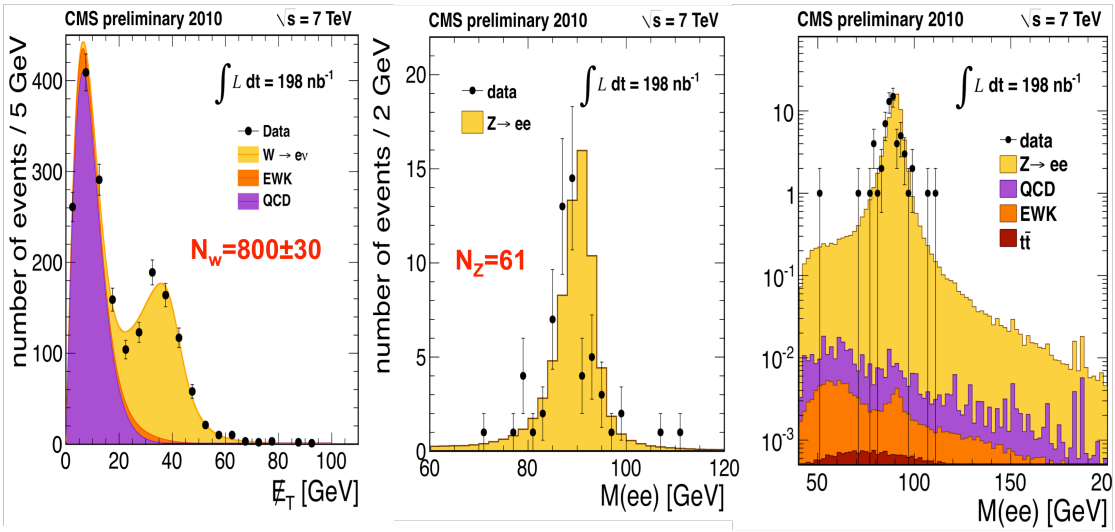

Fig.11 Transverse missing energy distribution for W→eν (left), and invariant-mass distributions for Z(γ)→e⁺e⁻, in linear (center) and logarithmic scale (right).*

We measure inclusive W and Z production cross sections in combined muon and electron decay channels at $\sqrt{s}$=7TeV to be $\sigma(pp\to W+X\to \ell\nu+X)=9.22\pm0.24(stat.)\pm0.47(syst.)\pm1.01(lumi.)$nb, and $\sigma(pp\to Z(\gamma^*)+X\to \ell^+\ell^-+X)=0.882+0.077-0.073(stat.)+0.042-0.036(syst.)\pm0.097(lumi.)$nb, where ℓ=e or μ. The uncertainty in the measurement is dominated by the 11% currently estimated error on the luminosity determination (Fig.12).

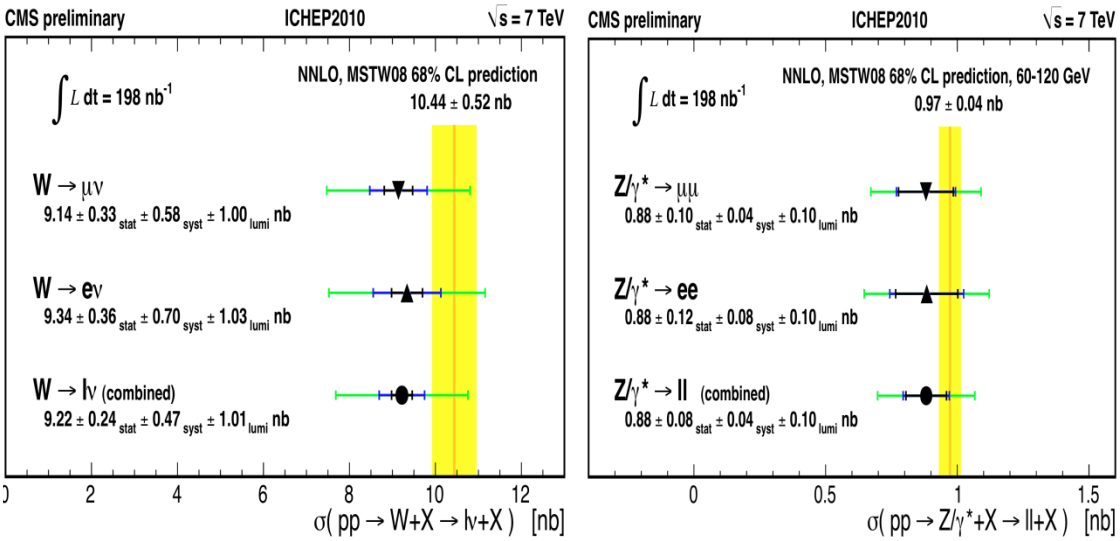

Fig.12 Inclusive W and Z cross sections in muon and electron decay channels.

The luminosity-independent cross section ratio W/Z is $\sigma(pp\to W+X\to \ell\nu+X)/\sigma(pp\to Z(\gamma^*)+X\to \ell^+\ell^-+X)=10.46\pm0.99(stat.)\pm0.65(syst.)$. Since the parton composition of the incoming protons favors the production of W^+, we have measured independently the W^+ and W^- inclusive production cross section and checked the luminosity independent cross section ratio $\sigma(pp\to W^++X\to \ell^+\nu+X)/\sigma(pp\to W^-+X\to \ell^-\nu+X)=1.51\pm0.08(stat.)\pm0.04(syst.)$. The measured values agree reasonably well with NNLO cross sections calculations and current parton distribution functions (Fig. 13).

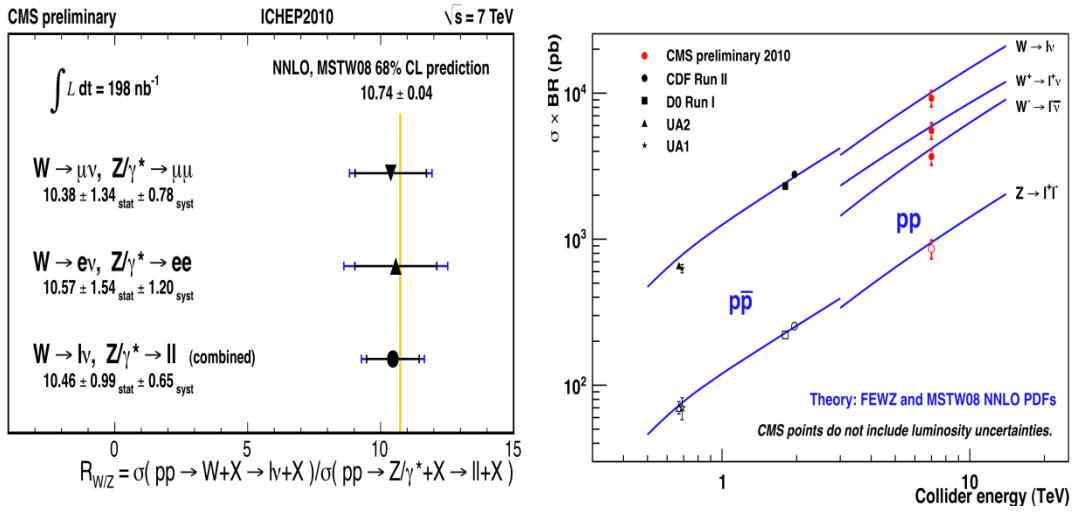

Fig.13 Ratio of W and Z inclusive cross sections in leptons (left) and comparison between the measured cross section values and NNLO predictions.

3.4 Top quark

The selection of top quark candidates is particularly challenging since it requires a complete understanding of all major physics tools. Top quark candidates were searched in CMS looking at channels with high p_T leptons or di-leptons, jets and missing E_T with at least 1 jet b-tagged. The selection in the lepton+jets channels starts from the data set produced using inclusive muon and electron triggers [$\mu+X$ (p_T >9GeV/c) or $e/\gamma+X$ (E_T>15GeV]. We first look for exactly one prompt, isolated electron (muon) of good quality using different p_T cuts for electrons and muons due to the different backgrounds: p_T(e)>30GeV/c, $|\eta_e|$<2.4 and $p_T(\mu)$>20GeV/c, $|\eta_\mu|$< 2.1. The selection of top candidates is then based on the presence of high missing transverse energy in the events [MET>30(20)GeV for e(μ)], and at least three jets in the events with one of them b-tagged with a simple secondary vertex tagger [13].

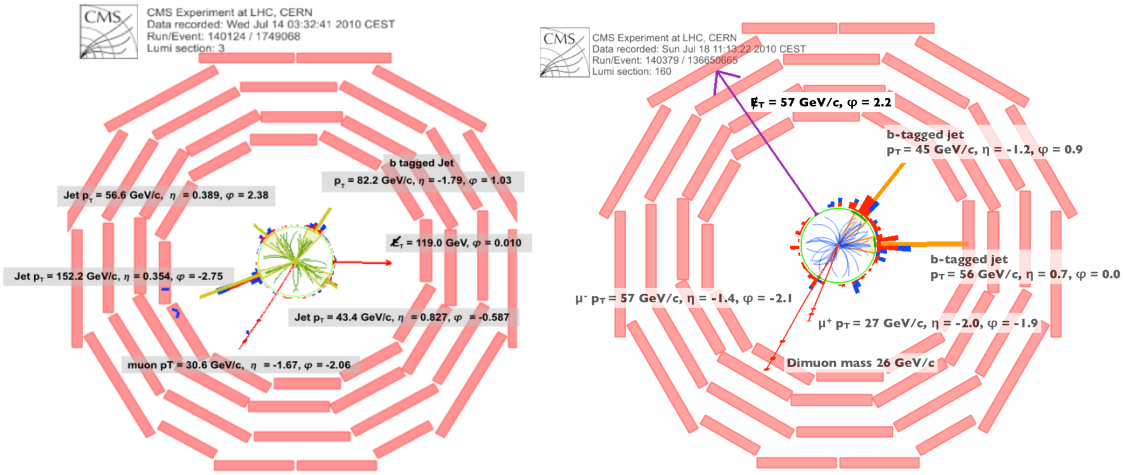

Fig. 14. Event displays of top quark candidates in high p_T leptons, jets and missing E_T (left) and high p_T di-leptons, jets and missing E_T (right). In both cases at least 1 jet is b-tagged.

The analysis in the di-leptonic channel is based on the same inclusive muon and electron triggers but data are selected requiring two isolated, prompt, oppositely charged leptons (l=e,μ) of good quality p_T(l)>20 GeV/c. Similar selection criteria are then used for the MET and for the presence of b-tagged jets in the event. We then apply a *Z*-boson veto, rejecting all events containing opposite-sign same-flavour di-leptons whose invariant mass is compatible with the Z hypothesis ($76<M_{ee,\mu\mu}<106$GeV/c^2). Typical event displays of top candidates are shown in Fig.14. The event display on the left shows the presence of a high-momentum muon ($p_T(\mu)$=30.6GeV/c), MET>100GeV and 4 high-p_T jets, one of which with good *b*-tag. A couple of possible combinations of missing E_T with the muon leading to a transverse mass compatible with the presence of a W in the event (m_T=104-105 GeV/c^2). The top quark candidate in the di-leptonic channel shown on the right contains two high p_T muons with opposite charge, two jets, both with secondary vertices (b-tagged) and a significant missing transverse energy (MET>50 GeV). The event passes all cuts of the selection for top candidates including the Z-veto ($M_{\mu\mu}$=26GeV/c^2); the preliminary reconstruction of the mass leads to a value in the range 160-220GeV/c^2, fully compatible with the top hypothesis.
Going through the full statistics collected so far, 254nb^{-1} and requiring at least 1 jet b-tagged in the event, it has been possible to produce the distributions shown in Fig. 15 for lepton+jets (left) and di-lepton events (right).

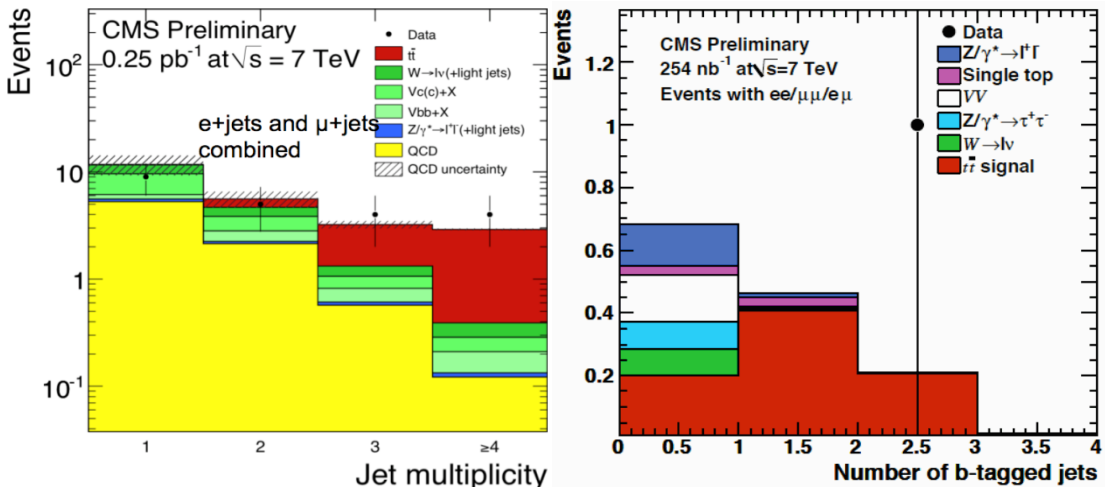

Fig. 15. Distribution the lepton+jets events as a function of jet multiplicity (left) and of the single di-lepton event candidate as a function of the number of b-tagged jets (right); both distributions are compared with Monte Carlo expectations for various backgrounds and t-tbar signal.

For the lepton+jets selection there is a good agreement between data and Monte Carlo expectations for the various sources of background. Fig. 15 (left) shows that top candidates events populate the bins corresponding to jet multiplicities ≥3 where one counts 8 events in the data over an expected background of less than 2. The single di-muon event passing the full di-lepton selection sits in a bin of the distribution as a function of b-tagged jets (Fig.15 right) where the background is practically negligible. We can therefore conclude that the first top quark candidate produced by LHC have been clearly identified within the CMS data. This is the first observation of top quark pairs produced in LHC data. As soon as additional statistics becomes available it would be possible to produce also the first preliminary measurement of the top quark production cross section at the LHC.

4. Conclusion

We have presented the status of the CMS experiment at the LHC and highlights of the first physics results obtained using pp collisions at 7TeV. We reported on the results of the commissioning of the main detector components and of the most important physics objects and tools.
We have presented the first results on charged hadrons multiplicities, on inclusive jet cross-sections and on the measurements of the J/ψ and ϒ differential cross section as a function of p_T.
We have shown results on W and Z bosons and preliminary measurements of their production cross-sections. Lastly we have presented the first observation of top quark pairs produced in LHC.
Having achieved so quickly a good understanding of the detector performance and of the Standard Model properties at 7TeV, we consider CMS to be ready to explore the new energy regime in the quest for signals of new physics.

Acknowledgements

I would like to thank first the LHC accelerator team for achieving an impressive performance of the machine in its first year of running. I am grateful to all colleagues of the CMS collaboration for their huge collective effort in constructing and running the experiment and analyzing so quickly and so efficiently data collected just up to a few days ago. Lastly I would like to thank the Organizers for making this Conference such an interesting and stimulating experience.

References

[1] CMS Collaboration, *The CMS Experiment at the CERN LHC*, ***JINST* 3** (2008) S08004.
[2] CMS Collaboration, *Measurement of CMS Luminosity*, **CMS-PAS-EWK-10-004** (2010).
[3] CMS Collaboration, *Tracking and Primary Vertex Results in First 7TeV Collisions*, **CMS-PAS-TRK-10-005** (2010).
[4] CMS Collaboration, *Commissioning of b-jet Identification with pp Collisions at √s=7TeV,* **CMS-PAS-BTV-10-001**(2010).
[5] CMS Collaboration, *Jet Performance in pp Collisions at √s=7TeV,* **CMS-PAS-JME-10-003** (2010).
[6] CMS Collaboration, *Missing Transverse Energy Performance in Minimum-Bias and Jet Events from Proton-Proton Collisions at √s=7TeV,* **CMS-PAS-JME-10-004** (2010).
[7] CMS Collaboration, *Transverse-momentum and pseudorapidity distributions of charged hadrons in pp collisions at √s=7 TeV,* ***Phys. Rev. Lett.* 105** (2010) 022002.
[8] The CMS Collaboration, *Measurement of the Inclusive Jet Cross Section in pp Collisions at 7TeV,* **CMS-PAS-QCD-10-011** (2010).
[9] CMS Collaboration, *Search for Dijet Resonances in the Dijet Mass Distribution in pp Collisions at √s=7TeV,* **CMS-PAS-EXO-10-001** (2010).
[10] CMS Collaboration, *J/ψ Prompt and Non-Prompt Cross Section in pp Collisions at √s=7TeV,* **CMS-PAS-BPH-10-002** (2010).
[11] CMS Collaboration, *Measurement of the Inclusive Upsilon Production Cross Section in pp Collisions at √s=7TeV,* **CMS-PAS-BPH-10-003** (2010).
[12] CMS Collaboration, *Measurements of Inclusive W and Z Cross Section in pp Collisions at √s=7TeV,* **CMS-PAS-EWK-10-002** (2010).
[13] CMS Collaboration, *Selection of Top-Like Events in the Dilepton and Lepton-plus-Jets Channels in Early 7TeV Data,* **CMS-PAS-TOP-10-004** (2010).